Available online at www.sciencedirect.com
SCIENCE DIRECT®
Journal of Human Evolution 44 (2003) 167–187

Cranial integration in *Homo*: singular warps analysis of the midsagittal plane in ontogeny and evolution

Fred L. Bookstein[a,b], Philipp Gunz[a], Philipp Mitteröcker[a], Hermann Prossinger[a], Katrin Schæfer[a*], Horst Seidler[a]

[a] *Institute for Anthropology, University of Vienna, Althanstrasse 14, 1091 Vienna, Austria*
[b] *Institute for Gerontology, University of Michigan, Ann Arbor, MI USA*

Received 15 March 2002; accepted 4 November 2002

Abstract

This study addresses some enduring issues of ontogenetic and evolutionary integration in the form of the hominid cranium. Our sample consists of 38 crania: 20 modern adult *Homo sapiens*, 14 subadult *H. sapiens*, and four archaic *Homo*. All specimens were CT-scanned except for two infant *H. sapiens*, who were imaged by MR instead. For each specimen 84 landmarks and semilandmarks were located on the midsagittal plane and converted to Procrustes shape coordinates. Integration was quantified by the method of *singular warps*, a new geometric-statistical approach to visualizing correlations among regions.

The two classic patterns of integration, evolutionary and ontogenetic, were jointly explored by comparing analyses of overlapping subsamples that span ranges of different hypothetical factors. Evolutionary integration is expressed in the subsample of 24 adult *Homo*, and ontogenetic integration in the subsample of 34 *H. sapiens.* In this data set, vault, cranial base, and face show striking and localized patterns of covariation over ontogeny, similar but not identical to the patterns seen over evolution. The principal differences between ontogeny and phylogeny pertain to the cranial base. There is also a component of cranial length to height ratio not reducible to either process. Our methodology allows a separation of these independent processes (and their impact on cranial shape) that conventional methods have not found.

Keywords: Cranial integration; Geometric morphometrics; Singular warps; Relative warps; Human ontogeny; Human phylogeny

Introduction

In the enduring debate about the tempo and mode of hominid evolution, one of the most helpful points of view is to emphasize integration, the interplay of trends and variability in the forms of components. Whereas biological hypotheses are statements of cause, findings of morphological integration pertain to the effects of those causes: the correspondence of patterns of covariation among traits to *a posteriori* or *a priori* hypotheses regarding factors such as evolution, development,

* Corresponding author

0047-2484/03/$ - see front matter
doi:10.1016/S0047-2484(02)00201-4

or function (Chernoff and Magwene, 1999). In this approach, which is embraced in the present paper as well, integration is assessed by the patterns of phenotypic statistical association within carefully designed samples intended to highlight the effects of the factor or factors postulated. The logic here corresponds to one version of Olson and Miller's (1951) "ρF-model", the comparison of empirically derived clusters of trait-measurements (ρ-groups) against sets of traits derived *a priori* from preconceptions or exogenous experimental observations about development and function (F-groups).

Olson and Miller (1958), in their classic book on morphological integration, eliminated the F-groups from their formal model; along with most other modern workers, we prefer the earlier formulation, in which biological theory takes priority over statistics. In our application the ρ's will be covariances rather than correlations and the F-sets will comprise coordinates of landmarks and semilandmarks in specific regions of the cranium. The use of regions as F-sets in this way goes back at least as far as Sewall Wright's original biometric factor analysis (reviewed in Bookstein et al., 1985).

In typical earlier applications, beginning with Olson and Miller's (1951) work, correlations between scalars (such as distances, ratios or angles) were used to challenge hypotheses about integration. These features needed to be listed in advance of any analysis, along with the specific patterns expected that would count as evidence for integrative factors of various types. Nowadays, we use landmark coordinates, not separately measured features, and hypotheses about integration are expressed as lists of landmarks, not lists of measured variables. When data are available as landmark coordinates over two or more regions, geometric morphometrics offers a multivariate technique that covers all possible shape measurements of the regions separately, exploring the patterns of their correlations with all possible shape measures of other regions in one single computation. The analysis results in lists of measures within a region that are optimally associated across regions. The lists emerge (somewhat as principal components do) in one single descending order of statistical explanatory power. The corresponding biological explanatory power arises from the geometrical or functional separations among the regions sent for analysis. Because the data set is one of landmark coordinates, the integrated features produced are interpretable as coordinated deformations over multiple regions, a more powerful diagrammatic tool, in general, than anything available in Olson and Miller's time.

Within any such explanatory setting, the investigator may be interested in the regionalizations claimed or in the explanatory factors. Our purpose in the present study is a hybrid of these two: to compare two distinct integrative factors, ontogeny and phylogeny, as they apply to a shared regionalization within one single sample of hominid crania. Studies of mammalian cranial development (Cheverud, 1982, 1995; Hanken and Hall, 1993; Moore, 1981) indicate that the skull is composed of several semiautonomous functional/developmental complexes. At the broadest scale, the skull is composed of three parts, the cranial vault, cranial base, and face (de Beer, 1937; Cheverud, 1996). Although they originate in embryologically distinct regions, they apparently grow in a morphologically integrated manner through numerous developmental and functional interactions (Lieberman et al., 2000a).

Particular attention has recently been paid to the role of the cranial base. The cranial base of anatomically modern *Homo* differs markedly from that of other primates and also is different from fossil *Homo*. Among the multitude of hypotheses that have been proposed to explain the high degree of midsagittal craniobasal flexion of anatomically modern *H. sapiens*, encephalization and facial orthognathism are the ones most often studied (Biegert, 1963; Dean, 1988; DuBrul, 1977; Gould, 1977; Jeffery and Spoor, 2002; Liebermann and McCarthy, 1999; Ross and Henneberg 1995; Ross and Ravosa, 1993; Strait, 1999). But such explanations are considerably weakened if the same methodology applies without alteration to both a study of ontogeny and a study of evolutionary change. As many measures of the hominid skull show the same trends over ontogeny as they do over phylogeny read backward, the differentiation of these two hypotheses is a matter of some delicacy. The methodology introduced here may

be construed as one that draws the greatest contrast between these two partial summaries. The contrast, in turn, may be interpreted as a heterochrony or heterotopy, or instead as a replacement of one ontogenetic pattern by another; we cannot pursue these further interpretative problems in the present data set.

Our specific purpose in this paper is to contrast the reports of one particular formal computation, singular warps analysis (see below), between two overlapping subsets of this sample, one filtered to highlight effects of an ontogenetic factor, and the other, those of a phylogenetic factor. We will show that these two factors, while quite similar in respect of the vault and the face, can be distinguished by close examination of their effects on the cranial base. The approach here differs in several particulars from that recently proposed by Lieberman et al. (2000b) for exploration of a similar but more focused question, the role of the cranial base in craniofacial integration. Our discussion below will begin with an exploration of the relation between their approach and ours. But first, of course, we introduce our methods, our data set, and our findings.

Material and methods

Specimens

We use a diverse cross sectional sample of modern and archaic *Homo* to study the large-scale effects of individual-level morphological integration. The sample was selected to cover a wide range of human shape variability. Our sample of 34 *H. sapiens* specimens consists of 20 adults of both sexes (nine from Central Europe, including Mladeč I (Szombathy, 1925), three San and two Bantu, three Chinese, two Australian aboriginals and one Papuan) and a cross sectional sample of fourteen European subadults ranging in age from 3 months to 17 years. The two youngest specimens (3 months and 9 months) were living children, measured from midsagittal slices of an MRI image. (CT scans of dried infant material are extremely difficult to quantify accurately, owing to their fragility and to the thinness of the bones even when imaged unbroken.) All other specimens were imaged using CT scans. In addition to these 34 *H. sapiens*, the sample included three Middle Pleistocene fossil *Homo* crania: Kabwe 1 (Broken Hill) (Woodward 1921), Petralona (Kokkoros and Kanellis, 1960), Atapuerca SH5 (Arsuaga et al., 1993), and one *H. neanderthalensis* cranium, Guattari 1 (Blanc, 1939).

Landmarks and preprocessing

Traditional landmarks were marked on each cranial CT in 3D, using the software package 3DViewnix (Udupa, 1999) in order to identify a midsagittal plane. The 18 unpaired landmarks (Table 1) were then projected onto this plane for each specimen and the corresponding slices exported as images. For the MRI scans the midsagittal slice was selected according to its unique anatomical properties (e.g. crista galli, aquaeductus mesencephali, septum pellucidum). Digitization of the landmark locations and capturing of the midsagittal outlines was done using tpsDig32 (Rohlf, 1998). All the coordinates were exported and processed with programs written in Mathematica®.

In addition to the anatomical landmarks (Table 1), 66 outline points were extracted along the inner and outer outlines of the vault and the midline of the maxilla. The outline points (including the landmarks *glabella*, *bregma* and *lambda*) were considered as *semilandmarks* free to slide along their curve-thus acquiring geometric homology within the sample (Bookstein et al., 1999). The 38 configurations of 84 points that resulted were averaged and represented as shape coordinates by standard Procrustes methods (Dryden and Mardia, 1998; Bookstein, 1997). Fig. 1 shows a typical midsagittal image with its 84 landmarks and semilandmarks.

A few landmarks are missing in some of the fossil specimens; these are indicated in Table 1. While the modern literature of missing landmark estimation (Gunz et al., 2002) emphasizes the statistical use of information from other forms, such procedures would obviously assume the fact of integration in essentially the same form in which we are testing it here; to avoid bias we therefore

Table 1
Definitions of landmarks (Martin and Saller, 1957; White and Folkens, 1991)

- rhinion (anterior free end of the internasal suture)
- nasion (the highest point on the nasal bones in the midsagittal)
- glabella (the most anterior point of the frontal in the midsagittal)
- bregma (the external intersection point of the coronal and sagittal sutures)
- 'internal bregma' (the point corresponding to bregma on the inside of the braincase)
- lambda (intersection of sagittal and lambdoidal sutures)
- 'internal lambda' (corresponding to lambda on the inside of the braincase)
- opisthion (midsagittal point on the posterior margin of the *foramen magnum*, **G**)
- basion (midsagittal point on the anterior margin of the *foramen magnum*, **G**)
- sella turcica (top of *dorsum sellae*, **P G**)
- canalis opticus intersection (intersection point of a chord connecting the two canalis opticus landmarks with the midsagittal plane, **P**)
- 'crista galli' (point at the posterior base of the crista galli)
- 'foramen caecum' (anterior margin of *foramen caecum* in the midsagittal plane)
- 'vomer' (sphenobasilar suture in the midsagittal plane)
- PNS 'posterior nasal spine' (most posterior point of the *spina nasalis*, **G**)
- 'fossa incisiva' (midsagittal point on the posterior margin of the *fossa incisiva*)
- 'alveolare' (inferior tip of the bony septum between the two maxillary central incisors)
- akanthion (top of the *spina nasalis anterior*)

Landmarks that were estimated in fossil specimens are indicated by initials.
G: Guattari, **P**: Petralona. The estimated landmark coordinates are available from the authors upon request.

could not use any of these novel tools. Missing landmarks were estimated with reference only to the single form upon which they were missing, by extrapolation of outline curves on midsagittal slices.

All our subsequent analyses require that the complete set of 84 points be divided into three subsets corresponding to the components the integration of which is to be discussed: cranial base, vault and face. These are indicated by color in Fig. 1. The neurocranium is traced up to a point that geometrically corresponds to Kabwe's occipital end (slightly above *inion*). Where landmarks lie on the interface between two functional components, we found (by experimenting) that it will not matter much to which they are assigned for the analyses to follow; we do not describe these alternative computations here.

Statistics

Multivariate analyses of this vector of 168 shape coordinates (two for each of the 84 landmarks and semilandmarks of the representation) were computed in two different approaches: relative warp analysis and singular warp analysis. As any discussion of integration must begin with a regional description, both computations do so; but whereas relative warp analyses refer to prediction of the shape of the craniofacial complex *as a whole*, the singular warp analyses refer to predictions of any of its components *from the other components*.

Relative warp analysis

Relative warp analysis, a modification of principal component analysis for shape coordinate data, is perhaps the most commonly encountered technique in the entire modern morphometric toolkit (Marcus et al., 1986; Bookstein, 1998; Corti et al., 2000; O'Higgins, 2000; Ponce de León and Zollikofer, 2001). A relative warp is an eigenvector of the matrix of variances and covariances of the Procrustes shape coordinates. When principal components are computed using covariances in this way, sums of squared differences of scores preserve the underlying original geometry of Procrustes distance.

Landmarks and semilandmarks can be mixed in this analysis, but the result depends on the relative density of landmark and semilandmark spacing (as

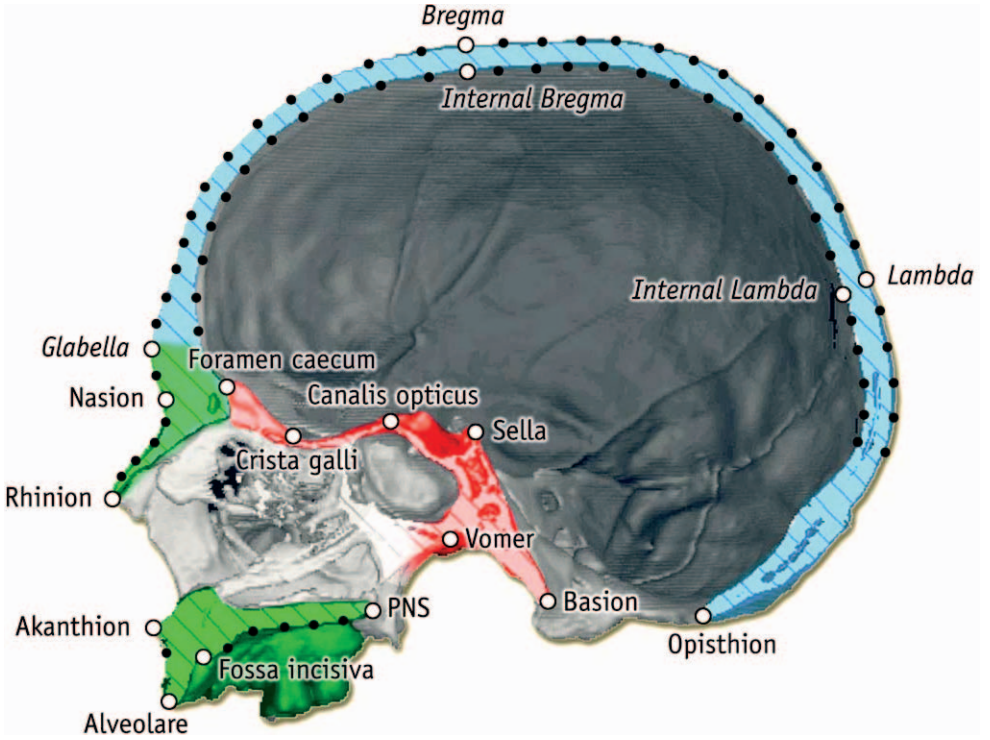

Fig. 1. Exemplary midsagittal image with 18 landmarks (open circles) and 66 semilandmarks (solid circles) assigned to the three defined regions: vault (blue), face (green), and cranial base (red). Semilandmarks and landmarks labelled in italics were free to slide along their curve. For definitions of the landmarks, see Table 1.

it varies over the cranium). Because this spacing was arbitrary (see Fig. 1) any report needs to impose some sort of standardization. From a variety of approaches to this problem we have chosen the simplest, a reweighting of the data so that vault, cranial base, and face appear to have the same net Procrustes leverage (point count). Algebraically, we have divided all the variances of the vault shape coordinates by 63, the count of vault points; all the variances of the cranial base shape coordinates by 6, the count of cranial base points; and all the variances of the facial shape coordinates by 15, the count of facial points. Vault-face covariances are thus divided by $\sqrt{63.15}$, vault-base covariances by $\sqrt{63.6}$, and face-base covariances by $\sqrt{15.6}$. After eigenextraction, the relative warps produced in this wise are "reinflated" by the appropriate multipliers before being visualized as transformation grids.

Singular warp analysis

Singular warp analysis is the name given to applications of Partial Least Squares (PLS) (cf. Bookstein et al., 1996) within morphometrics. This general class of techniques (Bookstein, 1998; Rohlf and Corti, 2000) involves a $N \times 2k$ matrix of shape coordinates X, and a $N \times m$ matrix of other variables Y, that may also be shape coordinates but need not be. A PLS analysis computes two unit vectors U_x^1, of length $2k$, and U_y^1, of length m, such that the covariance of XU_x^1 and YU_y^1 is a maximum. In words, these are the normalized composite scores (linear combinations), one from the X-variables and one from the Y-variables, that have the greatest mutual linear predictive power. Often a PLS analysis will go on to compute additional pairs of vectors U_x^2, U_y^2 for which U_x^2 is perpendicular to U_x^1 and U_y^2 is perpendicular to U_y^1 and the covariance of XU_x^2 and YU_y^2 is a maximum,

and so on. In general such multivariate vectors are called *singular vectors*; but, because when the *X*s are shape coordinates, each U_x can be visualized as a deformed or warped grid, they are usually referred to more specifically as *singular warps*. The adjective "singular" here is taken in the mathematical sense. [The reference is to the standard singular-value decomposition of the cross-block covariance matrix by which all of these composites may be computed at once (see Appendix and, for the algebraic theory, Mardia et al., 1979).]

For the analysis of integration reported here we have modified this "standard" singular-warp algorithm in two different ways. First, just as for the relative warp analysis, we have deflated the variance of each shape coordinate by the count of shape coordinate pairs in its anatomical component: a factor of 63 for the vault points, 6 for the base points, and 15 for the facial points. After deflation, these three candidate components affect one another, in principle, with equal weight, regardless of the differences in their point counts. Second, following the generalized algorithm of Streissguth et al. (1993), we have extended the analysis from two blocks to three blocks of shape coordinates, as indicated in the Appendix. The analysis set out in detail there results not in pairs but in triples of singular warps: one each for the vault, the base, and the face. Just as relative warps are supplied both as deformations (coefficients of how the shape coordinates jointly shift) and as scores, likewise singular warps are supplied both as deformations and as scores. Figs. 4–9 below show them in both aspects. Furthermore, because these are taken as linear combinations of the same unitary set of 168 Procrustes shape coordinates, they can be visualized as grids in two different ways: either separately, component by component, or jointly. The latter version incorporates the 'spaces between the components' as well as their deformations considered separately. They can be drawn as a composite spline because the components stay within the same Procrustes space throughout the whole analysis. Singular warps with negative covariances are reversed before drawing those summary figures. As far as we know, this visualization of the three singular warps as if they were one single relative warp has not been published previously. The diagrams generated by this device are remarkably suggestive.

Results

Relative warps

The relative warps were computed with $\alpha = 0$, i.e. with the uniform component included and no weighting by bending energy (Bookstein, 1996). A relative warps analysis is reported by the joint distribution of weighted scores together with the diagrams of the grid deformations corresponding to the eigenvectors that generated those scores. Fig. 2 shows the first two relative warps for the full dataset: all modern adults and children as well as the archaic ones, $N = 38$. (The Mladeč I cranium is within the range of modern *H. sapiens* shape variation throughout all these analyses, so for convenience it is *not* referred to as a fossil in this paper.)

Archaic *Homo* is separated from the moderns in the first relative warp (Fig. 2a), with the *H. sapiens* children at one extreme and the fossil specimens at the other. The grids of this first relative warp contrast the tall and large midface and thick vault-bones with large sinuses of the archaic specimens with the relatively small face of the modern children with thin vault bones and an almost spherical neurocranium (Fig. 2b). The grids visualizing the second relative warp contrast a prognathic and relatively elongated cranial shape with a retrognathic and tall cranial shape (Fig. 2b).

Singular warps

Even in its weighted version, the relative warps analysis is aimed at the aspects of these semilandmark configurations that are jointly most variable, while for interpretative purposes we are interested instead in the separate descriptions of vault, cranial base, and face and the relations between them. We therefore turn to the method of singular warps, and reanalyze two subsets of our full sample using this more pertinent method. With the one subset of all *H. sapiens* children and adults we analyze integration over an individual time

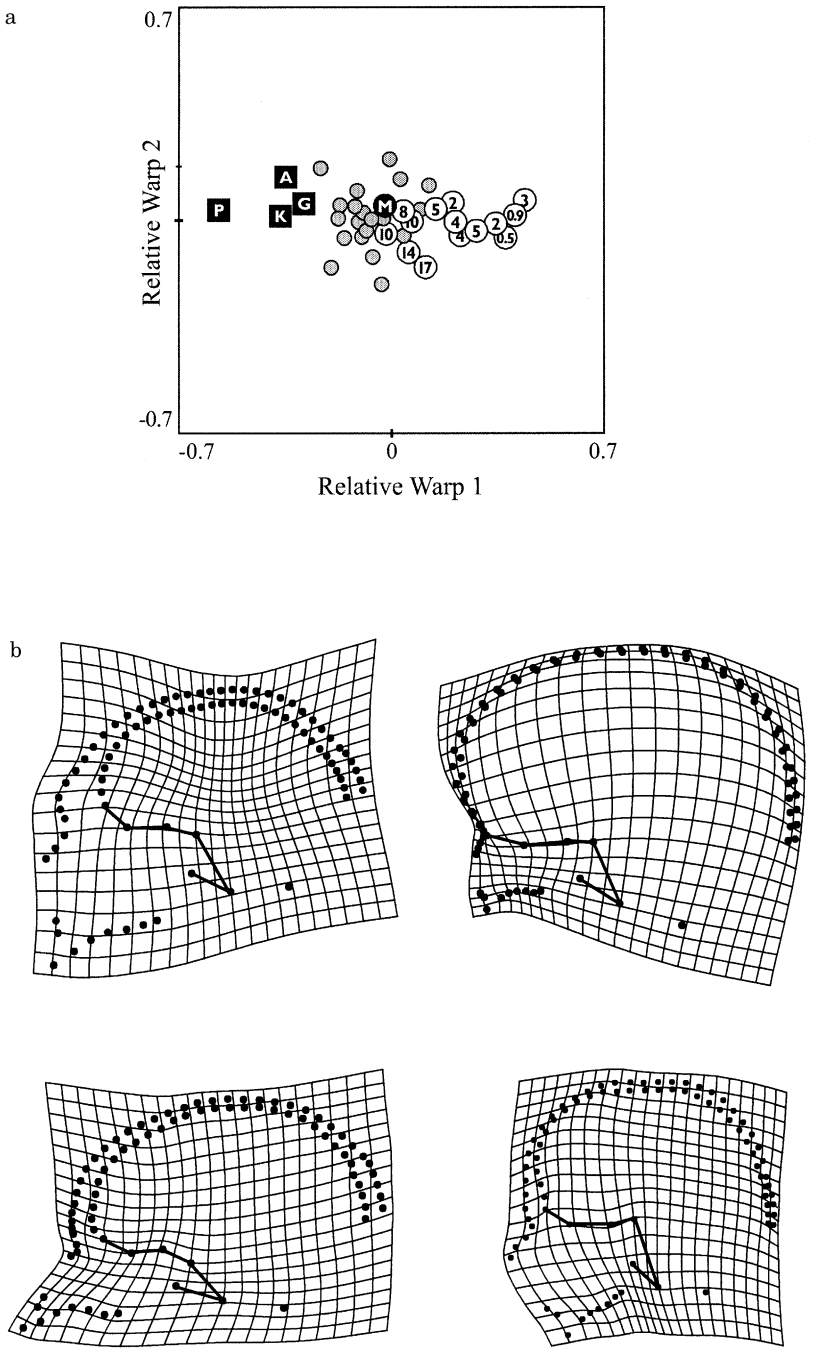

Fig. 2. Relative warps 1 and 2 for the full data set of 38 specimens. **(a)** Scatters of the sample keyed to the legend in the frame. Subadults are symbolized by age, fossils are indicated by initials, and the adult modern humans are unmarked. **M**: Mladeč, **G**: Guattari, **P**: Petralona, **A**: Atapuerca, **K**: Kabwe/Broken Hill. **(b)** Grids for the first two relative first warps (RW 1, RW 2) shown as deformations of the average in both directions. In this figure, correlated changes in geometric scale (Centroid Size) are not shown, and the magnitude of the contrasts on the RW's is arbitrary.

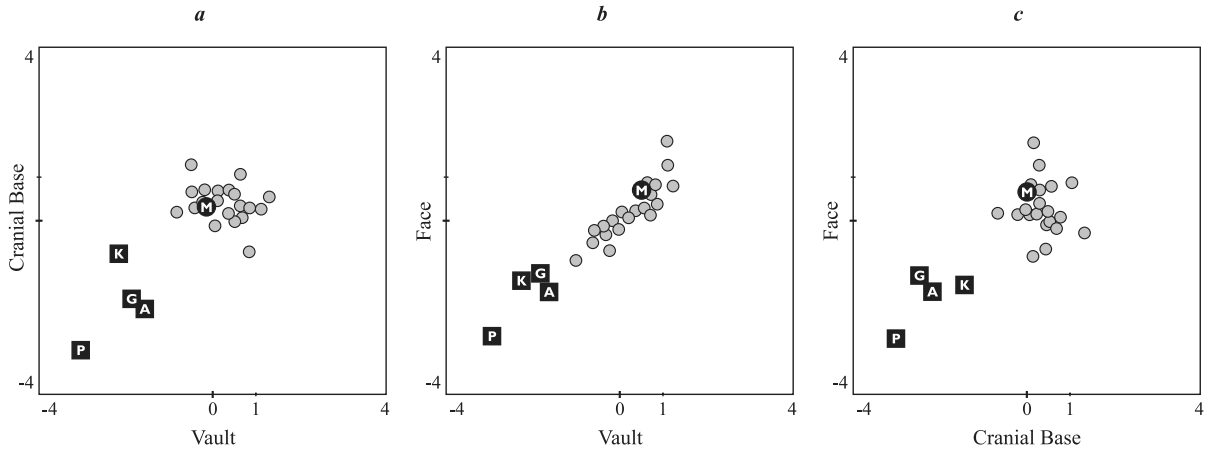

Fig. 3. *First* singular warp scores for the set of all adult *Homo* specimens ($N = 24$). **(a)** vault-cranial base, **(b)** vault-face, **(c)** cranial base-face. For legend, see Fig. 2. Archaic and modern *Homo* are clearly separated.

scale (ontogeny), while using the other subset of adult modern and archaic *Homo* we analyze integration over evolutionary time. The subsets overlap by 20 adult *H. sapiens.* But these specimens are ostensibly unvarying on both of the explanatory factors, ontogeny and phylogeny, which we intend to unravel. We will see, in fact, that they are subject to an unexpected factor of integration orthogonal to both. The analysis is not confounded, but rather enriched, by this overlap.

The singular warps can be visualized either using separate thin-plate-splines for vault, base and face or as one composite spline. The splines visualize the *patterns* of shape difference (the scales of the grids are arbitrary), while the plots of the singular warp scores show the contributions of each dimension to each actual shape.

Evolutionary integration

Figs. 3–6 deal with the singular warp analysis of the adult *Homo* subset ($N = 24$). Scores on the first dimension (Fig. 3) clearly separate archaic from modern *Homo*, but show a single linear trend in the covariation between vault and face, and a similar trend in the interaction of vault-base (Fig. 3a) and base-face (Fig. 3c). The composite spline (Fig. 4a) shows that the first singular warp of the adult *Homo*, like the first relative warp for the full sample, represents the shape difference of individuals with thin vault bones and relatively small faces versus robust individuals with relatively larger faces and sinuses and thick vault bones. The anterior cranial base is inclined downwards in the moderns (Fig. 4a,c) but upwards in the archaic shapes. Correlations of the singular warp scores: face with vault, 0.96; vault with cranial base, 0.68; face with cranial base, 0.71.

The second dimension of shape covariation among vault, base and face, Figs. 5 and 6, is by construction uncorrelated with the first dimension block by block (see Appendix). The grids (Fig. 5) show how this second singular warp corresponds to relatively tall versus relatively elongated crania, with the tall cranium incorporating the less prognathic face. There is a cranial base effect entailed also, as tall crania have a greater relative clivus length than elongated crania. In keeping with the adjustment of phylogeny (the first singular warp), the archaic specimens cannot be discriminated from the moderns in Fig. 6.

Developmental integration

We study ontogenetic effects in the *H. sapiens* subset ($N = 34$). The first singular warp scores (Fig. 7) exhibit a linear trend, children at one end and adults at the other. The corresponding splines

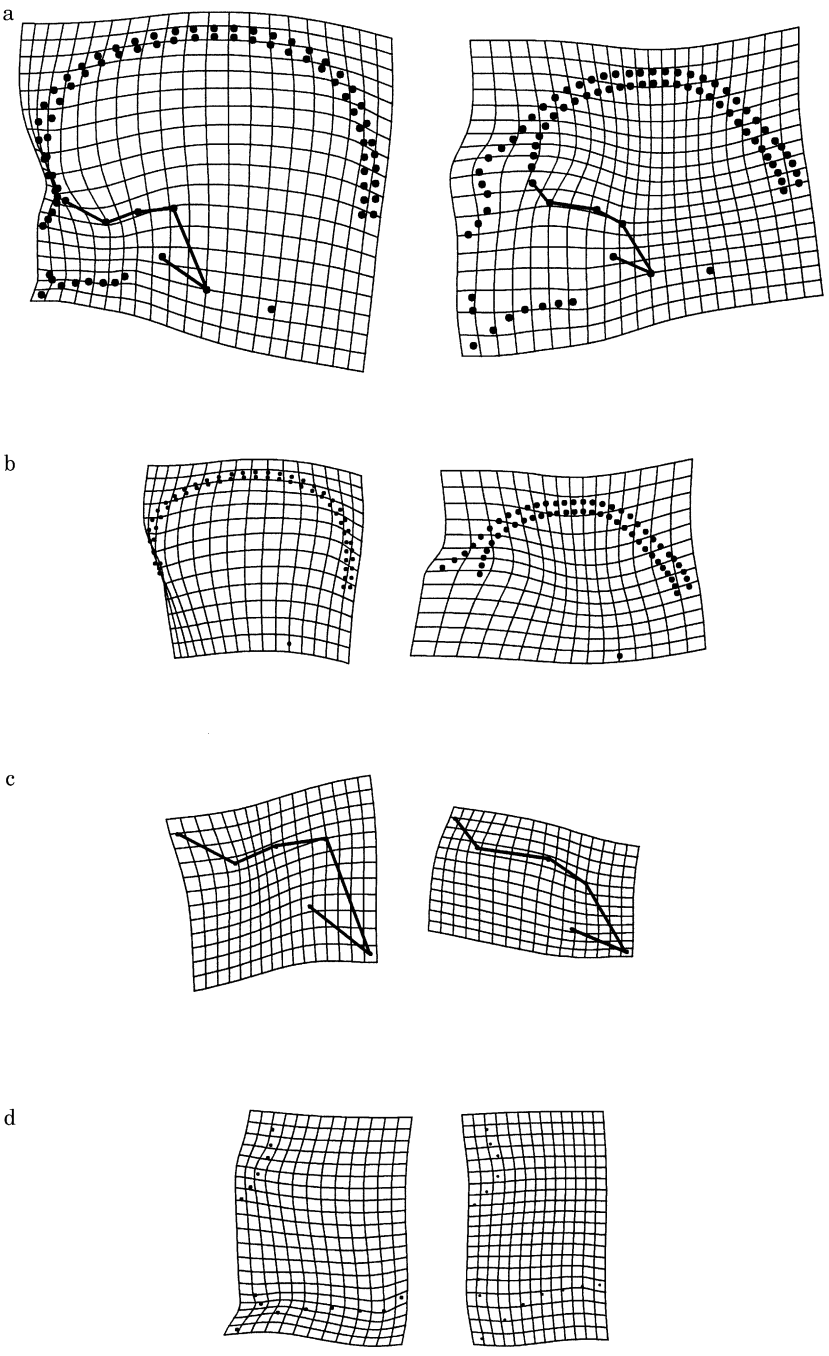

Fig. 4. *First* singular warp for the subset of all adult *Homo* specimens ($N = 24$): shown as a composite spline **(a)** and for each of the three blocks separately: **(b)** vault **(c)** cranial base and **(d)** face. Each of the pairs of grids represents both directions of deformation for the block involved. The three deformations of the left column are positively correlated, and likewise the right. Deformation toward the archaic (right column) represents the robust extreme of the forms with relatively larger faces and thicker vault bones. Deformation toward the modern specimens (left column) with a comparatively smaller face, relatively larger neurocranium, and thinner vault. Here and in all following figures, the magnitude of the contrasts on the singular warps that are shown as deformations is arbitrary.

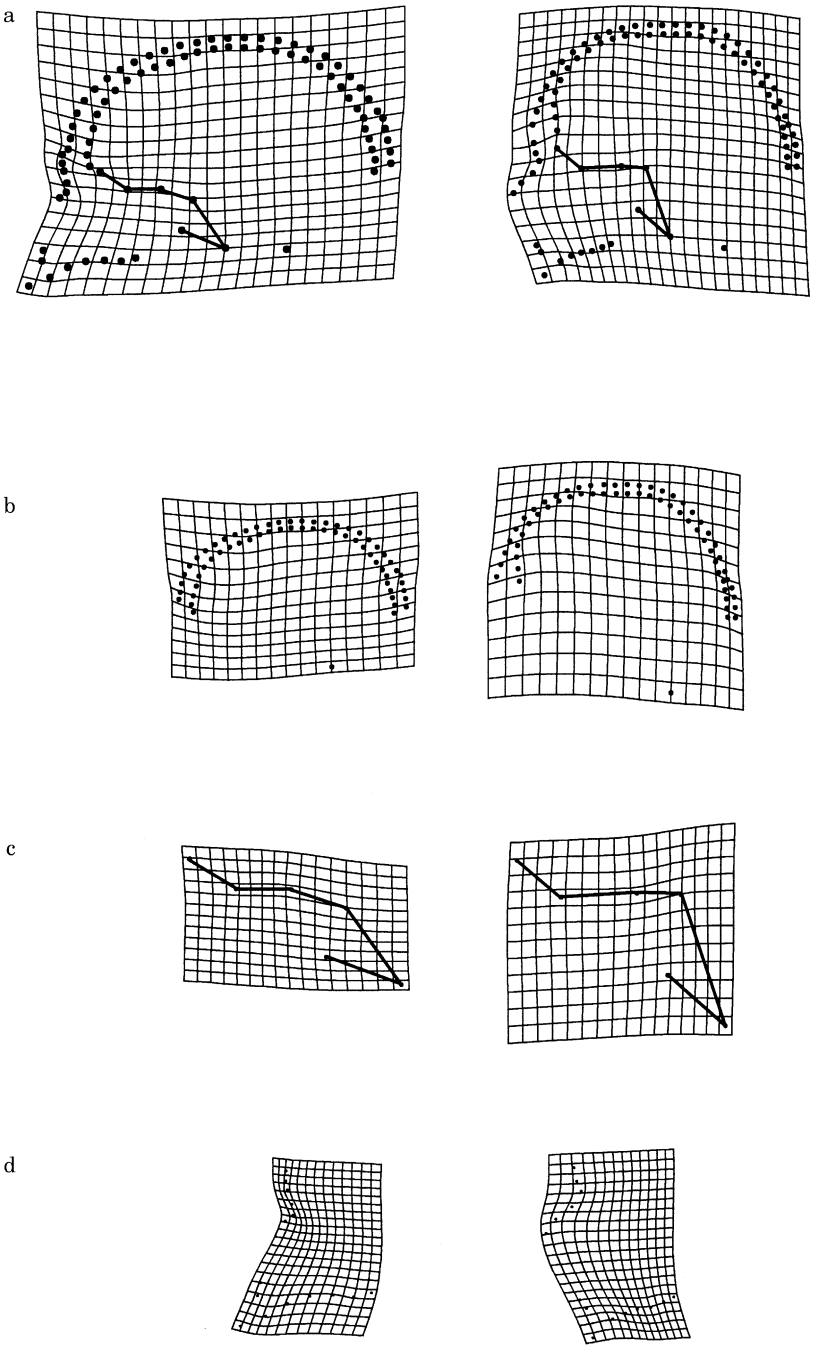

Fig. 5. *Second* singular warp for the subset of all adult *Homo* specimens ($N = 24$): composite **(a)** and separate splines **(b)–(d)**. Left column: Deformation of the average toward a longer cranial shape. Right column: Deformation toward a taller cranial shape.

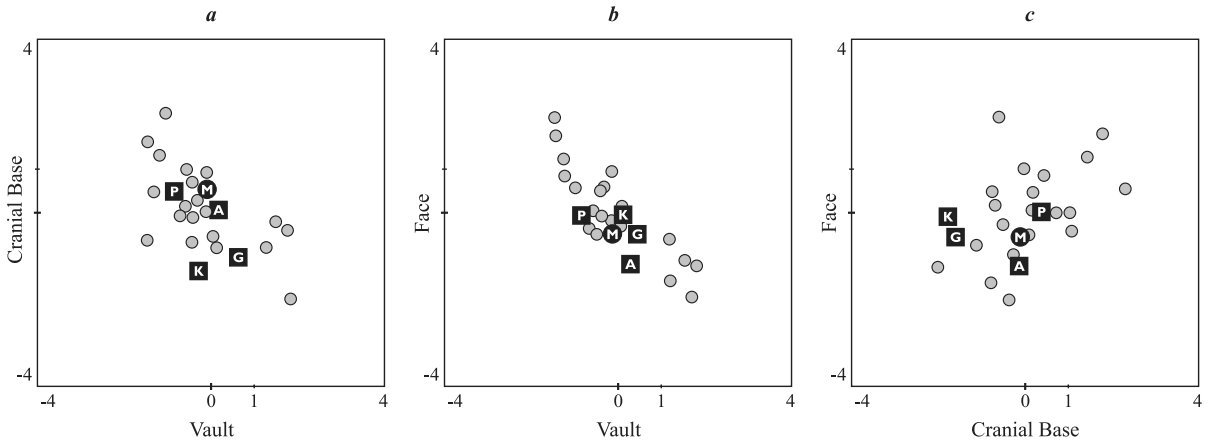

Fig. 6. *Second* singular warp scores for the set of all adult *Homo* specimens ($N = 24$). **(a)** vault–cranial base, **(b)** vault–face and **(c)** cranial base–face. Adult moderns and archaics do not separate. (For legend, see Fig. 2.)

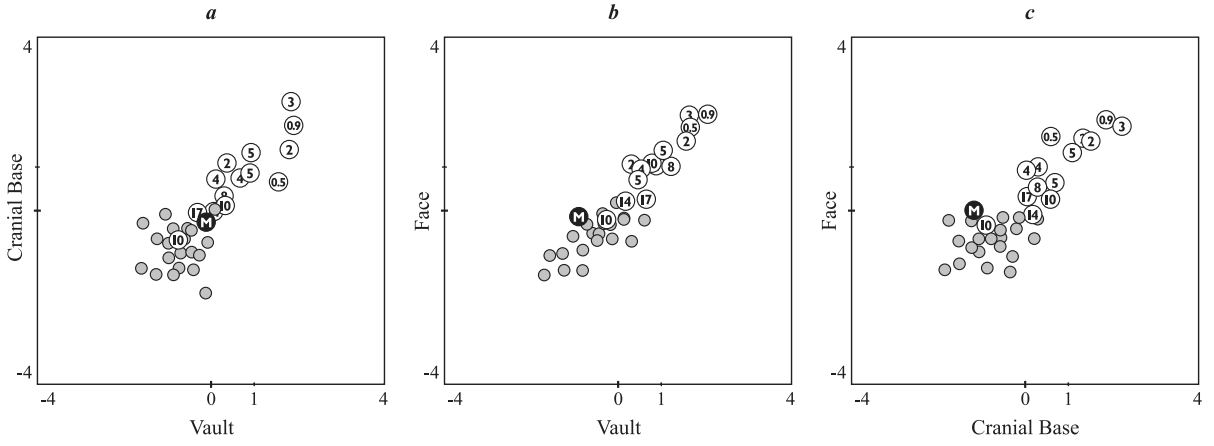

Fig. 7. *First* singular warp scores for the set of subadult and adult *H. sapiens* specimens ($N = 34$). **(a)** vault–cranial base, **(b)** vault–face and **(c)** cranial base–face. We find a linear trend for ontogeny. For legend, see Fig. 2.

in Fig. 8 show relative enlargement of the face and thickening of the vault during growth. The grids closely resemble the first singular warp of the adult *Homo* subset (Fig. 4), except in basicranial shape and in the angulation of the segment *prosthion–anterior nasal spine*. The ontogenetic shape changes of the cranial base differ markedly from the shape differences between modern and archaic *Homo*: The orientation of the anterior cranial base stays constant while vault and face alter their shape during ontogenetic development of *H. sapiens*.

Again, the second singular warp analysis expresses elongation or compression of the cranium (Fig. 9), and, as in the 2nd singular warp of the archaic-modern subsample; there is no correlation between age and singular warp scores in the ontogenetic subsample (Fig. 10). The shape of the vault is highly correlated with the shape of the face ($r \approx 0.9$). Crania with a tall vault also have relatively taller, more retrognathic faces than elongated crania. The relation of cranial length to height also influences the shape of the cranial base: The clivus is steeper in short cranial shapes.

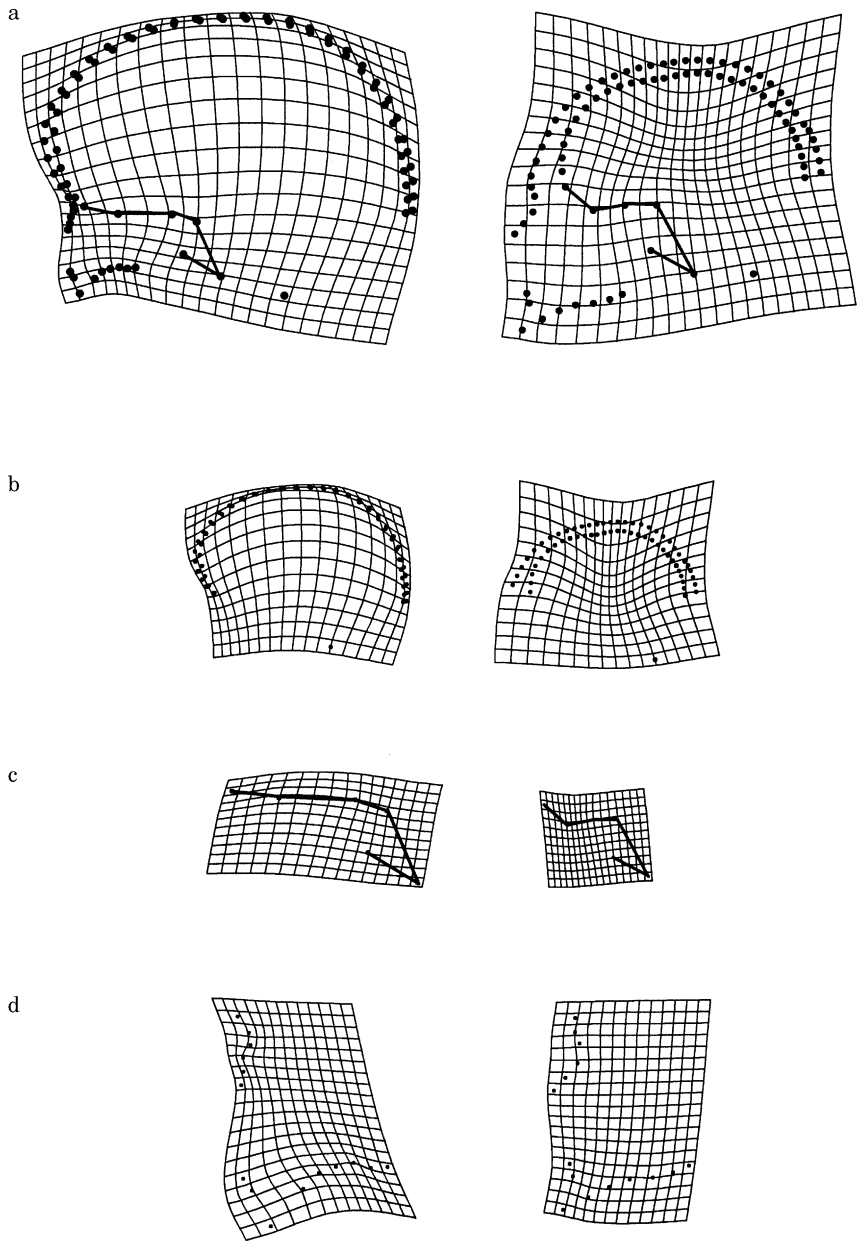

Fig. 8. *First* singular warp for set the of subadult and adult *H. sapiens* specimens ($N = 34$): composite **(a)** and separate splines **(b)–(d)**. Left column: Deformation from the mean form toward the infants. Right column: Deformation toward the adults.

Discussion

The grids illustrating shape differences of the first relative warp, which separates archaic and modern *Homo* (Fig. 2b), show an almost spherical braincase of modern *H. sapiens* compared to the elliptical vault of the fossil specimens (what Lieberman et al. (2002) term 'neurocranial globularity'), an overall decrease of bone thickness and facial reduction. This

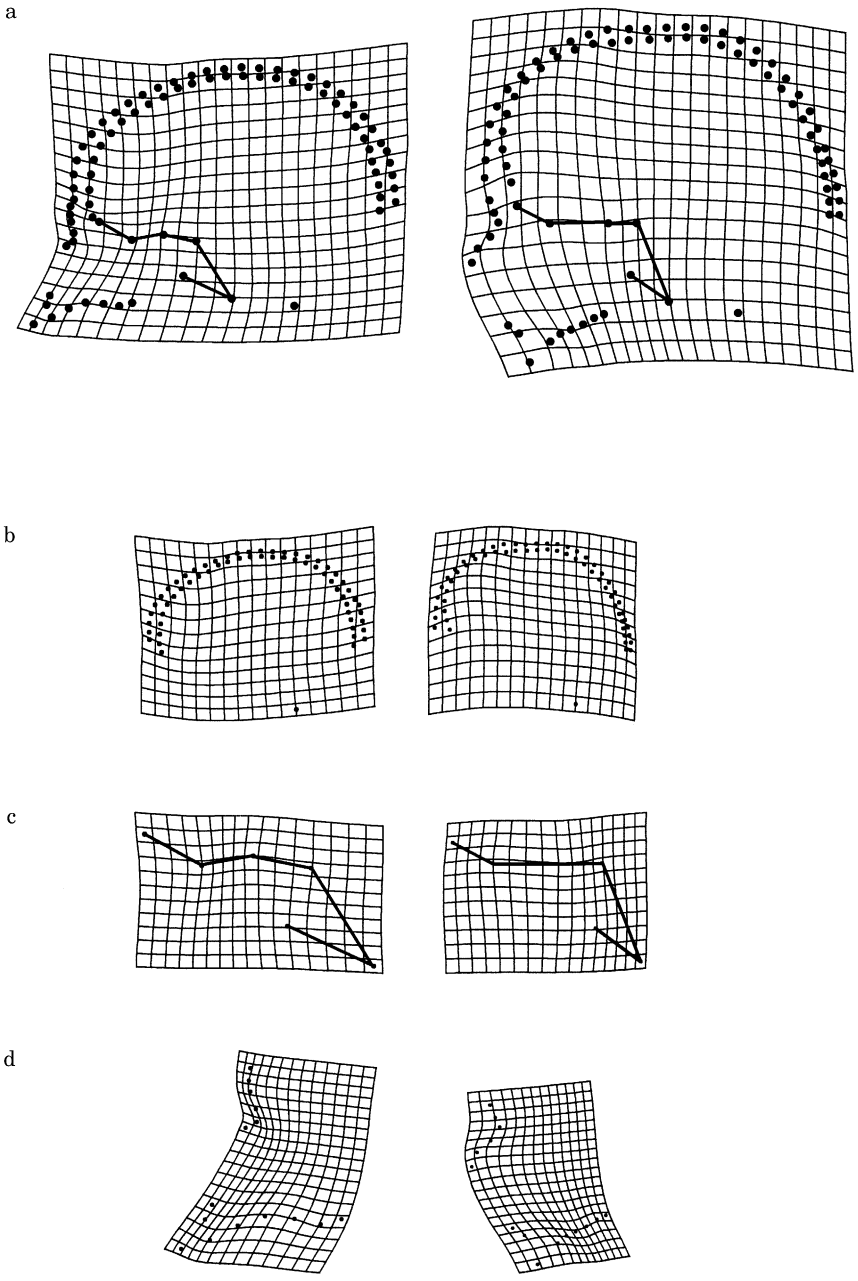

Fig. 9. *Second* singular warp for the set the of subadult and adult *H. sapiens* specimens ($N = 34$): composite **(a)** and separate splines **(b)–(d)**. Left column: Deformation toward a relatively elongated cranial shape; right column: Deformation toward a taller cranial shape. Similar deformations for the second singular warp were already identified in the subset of adult *Homo* (Fig. 5).

description has evidently omitted mention of the cranial base. It is the purpose of the singular warps analysis to partition the covariance in such a way that its changes are integrated with those of face and vault over two different subsets of the sample, the one emphasizing

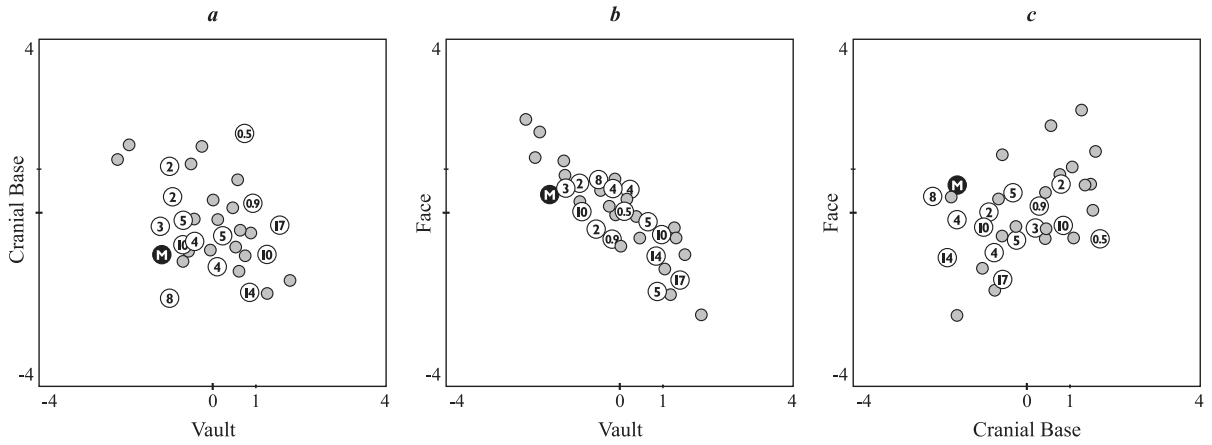

Fig. 10. *Second* singular warp scores for the set the of subadult and adult *H. sapiens* specimens ($N = 34$). **(a)** vault–cranial base, **(b)** vault–face, **(c)** cranial base–face. (For legend, see Fig. 2.) Adult and infant forms do not separate.

ontogenetic development, the other evolutionary change.

Methodology for studies of integration

The operationalization of integration by singular warps in this way differs somewhat from that of other recent publications. For instance, the useful review article by Lieberman et al. (2000a,b) notes, with ample citations, that "[integration is most basically revealed by complex patterns of correlation and covariation which indicate a lack of independence among variables … and which can be recognized a posteriori by comparing theoretically and empirically derived correlation matrices." [p. 161; citations omitted]

This paper goes on to set out, among the crucial issues on which "further research" is warranted, such concerns as the needs to "isolate and define the actual morphogenetic units which interact, to identify and quantify their direct and indirect interactions, and to understand the processes by which they interact" [p. 163]. In support of these goals, Lieberman et al. call for more data in three-dimensional form, on developmental mechanisms and especially the genetic basis of their variability, and on evolutionary implications of hypotheses like theirs. Along these lines, for instance Jeffery and Spoor (2002) study phylogenetic hypotheses of brain-cranial base interaction, where "interaction" is operationalized by way of correlations among size measures or between size measures and shape measures over ontogenetic series.

Our analysis has taken a somewhat different approach, in which, so to speak, the roles of theory and empirical data are interchanged. The "variables" that are taken for granted in the "basic" study of integration excerpted in the quotation from Lieberman et al. are replaced in our work by the configuration of landmark coordinates, within which the search for the specifically informative variables operationalized as the singular warps is in fact the main point of the investigation. And what Lieberman et al. treat as a comparison of one "empirically derived" covariance structure to another derived (somehow) from theory is here replaced by the comparison of two *different* empirical covariance structures, one expressing ontogeny, the other, evolution, each one operationalized by a structured subsampling of our data set as described earlier.

Furthermore, we accept the "actual morphogenetic units" in this study: the subdivision of the landmarks and semilandmarks in these three regions. In short, our work seems to take for granted nearly all the terms that are contested elsewhere in this literature, while concentrating on a straightforward methodological issue that seems to have been elsewhere overlooked: which measures of 'the

vault', 'the face', and 'the cranial base' should be taken to indicate their integration—each with the other components—and how the choice of these measures affects empirical claims that the finding of a correlation is pertinent to ontogeny, phylogeny, or something else. In terms of the quote from Lieberman et al., our concern is not with "lack of independence among variables" as pertinent to theory expressed *a priori*, but instead with the ways in which details of those dependences might shape interpretation *a posteriori*. In particular, processes that take place before the division into three components is established, or that take place explicitly upon the boundaries among these components, are not represented by the statistical methods introduced here. One version of the argument of this paper is that the same multivariate statistical methods support studies of integration as support studies of interaction, so that the distinction among these interpretations (between ontogenetic cause and evolutionary effect, as it were) needs to be carried out by a more careful differentiation of the pertinent data resources.

Besides this substitution of shape coordinates for variables, there is another redirection embedded in the approach we have taken: our implicit emphasis on the cognitive problem of what it means to "compare" one correlation matrix, perhaps "theoretical", to another, or to "quantify … direct and indirect interactions" among morphogenetic units. The method of singular warps is, in our view, a direct methodological construction that seems to carry out *both* of these descriptive purposes at the same time. The explicit quantification of "interactions" among vault, face, and cranial base in this midplane, carried out once to highlight phylogenetic variation and a second time for ontogenetic variation, serves simultaneously for the comparison of the corresponding covariance matrices to the extent they concern the integration of these three units.

It follows, we suggest, that the differences between these apparently distinct lines of research, one dealing with "integration" and the other with "interaction, " are not as central as hinted in the recent literature. If, in a morphometric context, the methods for the study of "interaction" and the methods for the study of "integration" are as overlapping as we are arguing them to be, then perhaps a different distinction is justified, between the design of the samples that permit empirical study of the integrated aspects of familiar biological processes (here, ontogeny and evolution) and the graphical language by which we can extract suggestions of the conventional descriptors (e.g., "globularity" or "length-to-height ratio") by means of which the necessary theoretical discussions of genetic and epigenetic origins can begin to be pursued. In other words, the method we have demonstrated here might serve as a bridge between data sets and the theoretical claims against which they have been previously tested only weakly, by statistical significance procedures. We believe that the graphical tests here are stronger, as we will show in the remainder of this discussion.

Such a use of multivariate analysis, which is generally referred to as "exploratory" (theory-generating rather than theory-confirming), has characterized biometry for most of the last century. We need not take the space to defend it, as it is so standard a complement to verificationist modes of reasoning in the same biometric toolkit. The differences we have displayed between pictures of ontogeny and phylogeny in the selfsame data set will be of great use in the further pursuit of Lieberman et al.'s goals for future work, by distinguishing what is to be explained by one theory from what is to be explained by others.

First singular warps: evolution and ontogeny

In the first singular warp, which expresses the patterns having the greatest covariation across the three components, the integration of vault with face over either evolution (Fig. 4) or ontogeny (Fig. 8) resembles the familiar combination of globularity with facial reduction in the relative warps of Fig. 2. Also, in both analyses the relative length of the clivus is increased. However, during ontogeny the Procrustes orientation of the anterior cranial base remains fixed (Fig. 8) whereas archaic and modern *Homo* differ by an obvious rotation of this component (Fig. 4).

The grids in Figs. 4 and 8 show the difference between integration over ontogeny and integration over phylogeny: features of face and vault that

have the highest covariance are nearly the same in the two patterns, but the manner in which this common factor embraces the cranial base is distinctive between the two explanations. The first singular warp of the adult *Homo* (Fig. 4) is correlated with facial reduction and neurocranial globularity as well as craniobasal flexion. In interpreting these grids, it is important to understand why these patterns do not translate correctly into restatements using conventional measurements such as "the cranial base angle". In both Figs. 4 and 8, the grid is actually quite inhomogeneous in the vicinity of the dorsum, so that the more appropriate description is that of a spatially localized change of the transformation, not the change of any single shape variable. The change in cranial base form in Fig. 4 (the singular warp for evolution, read in the direction of forward time, archaic to modern) incorporates an overall increase of vertical-to-horizontal ratio with a relative rotation "counterclockwise" of the anterior base from *dorsum* to *crista galli* and a relative repositioning of *canalis opticus* between *dorsum* and *crista*. The change in Fig. 8 (ontogeny, read from infant to adult) combines a similar increase of vertical-to-horizontal ratio and the same relative repositioning of *canalis opticus*, but incorporates no equivalent of the relative rotation of the anterior cranial base about *canalis*. There is also a local shift of *nasion* that is quite opposite between the two transformations. With these cranial base changes is associated an increase of neurocranial globularity over the archaic-to-modern transformation, but a decrease over the infant-to-adult transformation. The relative length of the clivus is increased in modern *Homo* (Fig. 4), when compared to the archaic specimens. This morphology emerges during postnatal ontogenetic development within the investigated time-range, as the children of our sample have a relatively shorter clivus than adults (Fig. 8).

Thus neither singular warp can be reported accurately as "change in the cranial base angle" or any other single familiar aspect of shape variation. Rather, they combine global and local aspects of shape change in partially similar and partially contrasting ways. Furthermore, changes in face and vault are much more strongly correlated with one another than either are with the cranial base feature changes, so that for statistical explanation of the evolutionary shape change no quantification of the cranial base alone could suffice. (As explained in Bookstein et al., 1985, in a single-factor model for three variables, the variable least correlated with the other two is also least correlated with the common factor.)

As one of us has noted elsewhere (Bookstein, 1994; Bookstein (2002)), in geometric morphometrics, shape variables come in a complete space of $2k-4$ dimensions (where k is the number of landmarks in two dimensions), within which it makes little sense to guess at the identity of useful variables *a priori*. Rather, the task of describing a hierarchy of contrasts of shape, such as a cladogram, lies primarily in the formulation of the *variables* in some principled manner. Shape variables that emerge from the contrast of two distinct integration patterns, as in this paper, are then to be tested as potential characters by the methods of Bookstein (2002) that take potential bifurcations of a cladogram explicitly into account in studies involving a larger subsample of archaic *Homo*.

That the singular warps call the observer's attention away from the cranial base angle *per se* does not mean that it might not prove important on other grounds arising, perhaps, from observations of earlier ontogenetic processes. The cranial base in *H. sapiens* flexes in a rapid trajectory that is mostly complete by about two years of age (Lieberman and McCarthy, 1999). Jeffery and Spoor (2002) have shown the cranial base to undergo several complex shape changes during prenatal development. As we have only two infant specimens, we cannot say more here about the complex integrative processes during gestation and the first postnatal years.

Second singular warps

The patterns described so far only constitute the first dimensions of singular warps (which means they account for the largest covariances between the three coordinate blocks). The second singular warps are the largest covariances between vault, base and face that are uncorrelated with the first singular warps. As we were able to interpret the first singular warps as evolution and ontogeny,

respectively, statistical independence means that the shape covariations of the second singular warps are related neither to ontogeny nor evolution, as can be seen in the overlap of archaic and modern specimens in the second singular warp for phylogeny (Fig. 6), or between young and adult specimens in the second singular warp for ontogeny (Fig. 10).

The grids of the second singular warp in both subsets (Figs. 5 and 9) look almost identical; both represent large scale variation in the height-to-length ratio of these crania. Accordingly, an elongated neurocranium is associated with a relatively short clivus and an obtuse basicranial angle, and a short, tall braincase with a relatively long clivus and an acute basicranial angle. Because archaic *Homo*, the modern adult and the modern subadult *H. sapiens* specimens completely overlap in the scatters of this second dimension, we consider this pattern to specify its own separate process of *Homo* cranial variation, orthogonal (by construction) to both ontogeny and phylogeny and also, apparently, unrelated to sexual dimorphism in this sample. It may be associated with heritable intrapopulation variation, epigenetic conditions, or some other morphogenetic explanation.

Although the second singular warp is uncorrelated with the first singular warp in the specific ontogenetic and phylogenetic samples segregated here, in any other sample there could be a component of this elongation to some variable extent, together with a tipping of the clivus associated neither with orthogenesis nor with growth but instead with the accidents of sampling on the elongation factor. Mixed samples combining these two processes will generally yield diagrams that combine the effects of all the processes contributing to the comparisons. To partial out this confounding, sample sizes would have to be so large as to be infeasible when dealing with fossil materials. Thus in comparisons across hominid evolutionary grades, changes in the cranial base angle *per se* as a single simple measurement should not be considered as separately interpretable aspects of either ontogenetic or phylogenetic integration. A report in terms of a cranial base angle, that is, some angle having *dorsum* as its vertex, would be appropriate only if the corresponding singular warp were fairly homogeneous in the vicinity of *dorsum* with principal strains bisecting that angle at dorsum (Bookstein, 1991, pp. 220–221). The necessary homogeneity does not obtain in either Fig. 4 or Fig. 8.

The overlap of archaic and modern specimens in the plots of the second singular warps scores bears implications for pro/retrognathism as a systematic character. Retrognathism is associated with both singular warps for both ontogeny and phylogeny: In ontogeny and evolution the size of the face changes relative to the neurocranium (SW 1) and taller crania have less prognathic faces (SW 2). Retrognathy is thus just as problematic a phylogenetic entity as cranial base angulation. Measures like these, so evidently expressing some process that is neither ontogeny nor phylogeny, should not be used for species discrimination within the genus *Homo*, as they tap some process of integrated variability that is unrelated to vault thickness, cranial or neurocranial volume, fossil age, or biological age. By contrast, a measurement like maxillary height loads on singular warp 1 but not on singular warp 2, and thus is a more promising candidate for a phylogenetically useful quantification.

Neurocranial globularity is a shape feature along the principal axis of variability and integration all across *Homo*: the feature expressed by this grid actually separates *H. sapiens* children from adults better than it separates *H. sapiens* adults from the fossil specimens. Hence we advise caution when considering this globularity as a systematic character.

Estimated landmarks

As noted in Table 1, two of the fossils in this paper incorporate a total of six missing landmark points. There is no evidence in either Fig. 3 or Fig. 6 that these two forms unduly affect the singular warp analysis of either vault or cranial base, but nevertheless the praxis by which these missing data were estimated deserves commentary. In general statistical practice, missing data is ordinarily estimated by some variant of the so-called 'EM algorithm'. Here 'EM' stands for "estimation/maximisation", a computation alternating between

(i) prediction of the individual missing data by a regression or analogous procedure based in the actual observations and (ii) fitting of the completed data set, estimated together with observed, to some population model such as a multivariate normal distribution. In morphometrics, special concerns such as symmetry or the need for smoothness of shape change factors add nuances to algorithms like these. When the scientific issue at hand is itself a study of integration, however, the treatment of missing data needs to be carefully adjusted so as not to presume what is actually to be demonstrated from the data. In the present study, the concern is with the large-scale covariances among vault, cranial base, and face; and so missing data needed to be estimated by reference to aspects of form that were not included in the covariance structure themselves and that were at a geometric scale smaller than that of the processes we were actually studying. The visual extrapolation of mesoscale curvatures in the midsagittal bony surface is one suitable praxis for this purpose. We have not estimated any large-scale aspects of these fossil forms, which are nearly complete as they stand; in particular, we have not extrapolated outside the boundary of the actual locations observed. Our method of missing data estimation thus permits us to include both Petralona and Guattari in the analysis, giving the findings somewhat greater scope without biasing them in any way.

Note that the computation here ordinates the Petralona specimen at one end of an imputed dimension-it is 'the most archaic' of the four crania. Furthermore, its singular warp scores are equally extreme in terms of vault and face, neither of which was missing any landmarks, nor in terms of the base, on which both landmarks from the sphenoid are missing. There is thus evidence that the estimated positions of those missing landmarks are consistent with the rearrangements of vault and face shape that are present in the actual data, even though neither vault nor face was involved in the estimation of these missing points. Regarding Guattari, which is missing three landmarks on the base, our single-image estimate leaves it located quite similarly in all three of the singular warp score scatters, Fig. 3. There is no evidence that the missing-data estimation has biased our results, although of course more complete specimens, and also more numerous fossils, would surely strengthen the argument.

Summary

Integration of the hominoid skull has long been a subject of active research in paleoanthropology and auxology. This paper adapts one of the classic approaches to integration, Olson and Miller's ρF-sets, to the modern context of geometric morphometrics. Analyses of the integration of cranial vault, base, and face over our mixed ontogenetic/phylogenetic sample of 38 hominid crania in midsagittal section show that these two processes, while equivalent in their morphological expressions in vault and face, can be distinguished by the patterns of their correlated effects on the cranial base. The description of this distinction involves relative clivus length and anterior cranial base orientation. Traditional measurements of the cranial base angle do not distinguish effectively between these ontogenetic and phylogenetic contexts of integration, nor between either of these and a third integrative process, involving relative elongation of the cranium across all three components, that is orthogonal to both ontogeny and phylogeny in this sample. The posterior cranial base is strongly influenced by the overall shape of the cranium. These independent sources of variation cannot be teased apart by one single angular measurement; furthermore, as vault and face summary scores correlate better with each other than either does with the cranial base, no set of cranial base features is likely, by itself, to suffice to explain evolutionary shape changes. We recommend that future analyses of integration use singular warps in preference to traditional measures of distance or angle so as to circumvent these and similar potential interpretative pitfalls.

Acknowledgements

We thank the curators of the fossil *Homo* crania, the subadult *H. sapiens* crania, and the adult *H. sapiens* crania for permission to CT-scan

them. Likewise we thank Wolfgang Recheis (Dept. of Radiology II, University Hospital Innsbruck, Austria) for CT-scanning support and Gerhard Weber (Institute for Anthropology, University of Vienna, Austria) for the installation and management of the digital database. We also thank Ingeborg Hirsch, Christine Unteregger and Barbara Wimmer for help with the data collection and Bence Viola and Dennis Slice for valuable discussions. This paper benefited greatly from the critical comments of three anonymous reviewers. This research is supported by the Austrian Federal Ministry of Education, Science and Culture and the Austrian Council for Science and Technology, Project Number: GZ 200.049/3-VI/I/2001.

Appendix. Algebra of two- and three-component singular warp analysis

The two-block PLS analysis reviewed in the main text is usually generated from the singular-value decomposition (SVD) of the cross-covariance matrix $\Sigma=(1/N)X^tY$ for two matrices of variables X: $N\times p$ and Y: $N\times q$ on the same sample. The SVD expresses the matrix $\mathbf{\Sigma}$ uniquely as $U_xDU_y^t$, where $U_x(p\times p)$ and $U_y(q\times q)$ are orthogonal matrices and $D(p\times q)$ is diagonal with elements in descending order. Then the first pair of singular vectors referred to in the text are the first column of U_x and the first column of U_y, and the covariance of XU_x^1 and YU_y^1 is the first element of D. The second pair of singular vectors combines the second column of U_x with the second column of U_y; the covariance of the corresponding scores is the second entry of D; and so on.

For the extension to more than two blocks there is no such standardization of the problem description. Rather, there arise a variety of different algorithms, each corresponding to one of the theorems that characterize the SVD in the classical two-block case. In addition to the maximum-covariance criterion cited in the main text, four other criteria are often encountered.

1. The singular vectors U_x are the principal components of the matrix $\mathbf{\Sigma\Sigma}^t$, and the singular vectors U_y the principal components of $\mathbf{\Sigma}^t\mathbf{\Sigma}$. The elements of D are the square roots of the eigenvalues of either of those symmetric matrices.
2. The dyadic product $D_1U_x^1(U_y^1)^t$ is the best rank-1 least-squares fit to the matrix $\mathbf{\Sigma}$; the sum, $D_1U_x^1(U_y^1)^t+D_2U_x^2(U_y^2)^t$,the best rank-2 approximation, and so on.
3. The vectors U_x^1, U_y^1, arise upon indefinite iteration of the sequence of matrix multiplications $U_x=\mathbf{\Sigma}U_y$, $U_y=\mathbf{\Sigma}^tU_x$, starting from almost any arbitrary U_x or U_y.
4. The coefficients of each singular vector, say U_x, are proportional to the regression coefficients of all the variables of the X-block on the score YU_y representing the singular vector of the Y-block and vice-versa.

To generalize all of this to the case of three or more blocks of variables, for instance the three cranial components of the application here, it is necessary to select one of these characterizations for extension; they no longer specify the identical computation. We have chosen, following Streissguth et al. (1993), to extend algorithm 3, the iterative matrix multiplication (but the other approaches lead to very similar findings). Write X_v, X_b, X_f for the centered deflated shape coordinate data of *v*ault, cranial *b*ase, and *f*ace.

Let U_v, U_b, and U_f be any three arbitrary guesses at the singular warps of these blocks. The algorithm that produced the findings here then loops over the following chain of computations:

Interpret U_v, U_b, and U_f as linear combinations; that is, compute scores

$$s_v = X_vU_v$$
$$s_b = X_bU_b$$
$$s_f = X_fU_f$$

and normalize each s to sample variance 1.

Compute the correlations among these scores in pairs:

$$r_{vb} = \mathrm{corr}(s_v, s_b)$$
$$r_{vf} = \mathrm{corr}(s_v, s_f)$$
$$r_{bf} = \mathrm{corr}(s_b, s_f)$$

Finally, compute updated estimates of the U's by summing predictions of the individual variables

(shape coordinates) using combinations of the scores s with the correlations r as weights:

$$U_v \leftarrow X_v^t(r_{vb}s_b + r_{vf}s_f)$$
$$U_b \leftarrow X_b^t(r_{vb}s_v + r_{bf}s_f)$$
$$U_f \leftarrow X_f^t(r_{vf}s_v + r_{bf}s_b)$$

and return to the top of the loop until the iteration has converged to the level of accuracy you demand.

At convergence, each singular warp is the pattern of deformation (that is, the profile of simultaneous shape coordinate shifts) predicted by the weighted combination of the other two singular warp scores for the joint shift of each shape coordinate simultaneously. (This generalizes the fourth in the list of characterizations of the ordinary two-block SVD above.)

We also modified the definition of subsequent singular warps. In the usual approach, the second and higher singular warps are orthogonal to the first as vectors. In the approach here, the second and higher singular warp *scores* are uncorrelated with the first as scalars. This permits the extraction of the truly uncorrelated dimensions of integration (statistically independent processes). The second SW triple is computed by applying the same algorithm to the residuals after the first SW triple is regressed out of each shape coordinate.

References

Arsuaga, J.-L., Martinez, I., Gracia, A., Carretero, J.M., Carbonell, E., 1993. Three new human skulls from the Sima de los Huesos. Nature 362, 534–537.

de Beer, G.R., 1937. The Development of the Vertebrate Skull. Oxford University Press, Oxford.

Biegert, J., 1963. The evaluation of characteristics of the skull, hands and feet for primate taxonomy, in: Washburn, S. (Ed.), Classification and Human Evolution. Aldine, Chicago, pp. 116–145.

Blanc, A., 1939. L'uomo fossile del Monte Circeo. Un cranio neandertaliano nella Grotta Guattari a San Felice Circeo. Atti Acad. Naz. Lincei Rc. Ser. 6 29, 205–210.

Bookstein, F., 1991. Morphometric Tools for Landmark data: Geometry and Biology. Cambridge University Press, New York.

Bookstein, F.L., 1994. Can biometrical shape be a homologous character? in: Hall, B.K. (Ed.), Homology: The Hierarchical Basis of Comparative Biology. Academic Press, San Francisco, pp. 198–229.

Bookstein, F., 1996. Combining the tools of geometric morphometrics, in: Marcus, L.F., Corti, M., Loy, A., Naylor, G.J.P., Slice, D (Eds.), Advances in Morphometrics. Plenum Press, New York.

Bookstein, F.L., 1997. Landmark methods for forms without landmarks: localizing group differences in outline shape. Med. Image Anal. 1, 225–243.

Bookstein, F.L., 1998. A hundred years of morphometrics. Acta Zool. Hung. 44, 7–59.

Bookstein, F.L., Chernoff, B., Elder, R.L., Humphries, J.M. Jr., Smith, G.R., Strauss, R.E., 1985. Morphometrics in Evolutionary Biology, Special Publication 15. Academy of Natural Sciences Press, Philadelphia.

Bookstein, F., Sampson, P.D., Streissguth, A.P., Barr, H.M., 1996. Exploiting redundant measurement of dose and developmental outcome: New methods from the behavioral teratology of alcohol. Dev. Psychol. 32, 404–415.

Bookstein, F., Schäfer, K., Prossinger, H., Seidler, H., Fieder, M., Stringer, C., Weber, G.W., Arsuaga, J.-L., Slice, D., Rohlf, F.J., Recheis, W., Mariam, A.J., Marcus, L.F., 1999. Comparing frontal cranial profiles in archaic and modern *Homo* by morphometric analysis. Anat. Rec. (New Anat.) 257, 217–224.

Bookstein, F.L., 2002. Creases as morphometric characters, in: MacLeod, N., Foley, P.L. (Eds.), Morphology, Shape and Phylogeny, Systematics Association Special Volume 64. Taylor and Francis, London, pp. 139–164.

Broom, R., 1947. Discovery of a new skull of the South African ape-man, Plesianthropus. Nature 159, 672.

Chernoff, B., Magwene, P., 1999. Morphological integration: forty years later, in: Olson, E., Miller, R. (Eds.), Morphological Integration. University of Chicago Press, Chicago, pp. pp. pp. 319–348.

Cheverud, J., 1982. Phenotypic, genetic, and environmental integration in the cranium. Evolution 36, 499–516.

Cheverud, J., 1995. Morphological integration in the saddle back tamarin (*Saguinus fuscicollis*) cranium. Am. Nat. 145, 63–89.

Cheverud, J., 1996. Developmental integration and the evolution of pleiotropy. Am. Zool. 36, 44–50.

Corti, M., Marcus, L., Hingst-Zaher, E. (Eds.), 2000. Geometric Morphometrics in Mammalogy. Hystrix 11, 1–154.

Dean, M., 1988. Growth processes in the cranial base of hominoids and their bearing on morphological similarities that exist in the cranial base of *Homo* and *Paranthropus*, in: Grine, F. (Ed.), Evolutionary History of 'Robust' Australopithecines. Aldine de Gruyter, New York, pp. 107–112.

Dryden, I.L., Mardia, K.V., 1998. Statistical Shape Analysis. Wiley, Chichester (UK).

DuBrul, E., 1977. Early hominid feeding mechanisms. Am. J. Phys. Anthropol. 47, 305–320.

Gould, S., 1977. Ontogeny and Phylogeny. Belknap Press, Cambridge.

Gunz, P., Mitteröcker, P., Bookstein, F.L., Weber, G.W., 2002. Approaches to missing data in anthropology. Coll. Antropol. 26, 78–79.

Hanken, J., Hall, B., 1993. The Skull, Development. Vol. 1. University of Chicago Press, Chicago.

Jeffery, N., Spoor, F., 2002. Brain size and the human cranial base: a prenatal perspective. Am. J. Phys. Anthropol. 118, 324–340.

Kokkoros, P., Kanellis, A., 1960. Découverte d'un crâne d'homme paléolithique dans péninsule Chalcidique. L'Anthropologie 64, 132–147.

Lieberman, D.E., McCarthy, R.C., 1999. The ontogeny of cranial base angulation in humans and chimpanzees and its implications for reconstructing pharyngeal dimensions. J. Hum. Evol. 35, 487–517.

Lieberman, D.E., Pearson, O.M., Mowbray, K.M., 2000a. Basicranial influence on overall cranial shape. J. Hum. Evol. 38, 291–315.

Lieberman, D.E., Ross, C.F., Ravosa, M.J., 2000b. The primate cranial base: ontogeny, function, and integration. Yearb. Phys. Anthropol. 43, 117–169.

Lieberman, D.E., McBratney, B., Krowitz, G., 2002. The evolution and development of cranial form in *Homo sapiens*. Proc. Natl. Acad. Sci. USA 99, 1134–1139.

Marcus, L.F., Corti, M., Loy, A., Naylor, G.J.P., Slice, D.E., 1996. Advances in Morphometrics. Plenum Press, New York.

Mardia, K.V., Kent, J.T., Bibby, J.M., 1979. Multivariate Analysis. Academic Press, London.

Martin, R., Saller, K., 1957. Lehrbuch der Anthropologie. Gustav Fischer, Stuttgart. pp. 488–490.

Moore, W., 1981. The Mammalian Skull. Cambridge University Press, Cambridge.

O'Higgins, P., 2000. Quantitative approaches to the study of craniogacial growth and evolution: advances in morphometric techniques. Development, Growth and Evolution. Academic Press, San Diego.

Olson, E., Miller, R., 1951. A mathematical model applied to a study of the evolution of species. Evolution 5, 325–338.

Olson, E.C., Miller, R.L., 1958. Morphological Integration. University of Chicago Press, Chicago.

Ponce de León, M.S., Zollikofer, C.P.E., 2001. Neanderthal cranial ontogeny and its implications for late hominid diversity. Nature 412, 534–538.

Rohlf, F.J., 1998. tpsDig32: A Program for Digitizing Landmarks and Outlines for Geometric Morphometric Analyses. Department of Ecology and Evolution, State University of New York, Stony Brook, New York.

Rohlf, F.J., Corti, M., 2000. The use of two-block partial least-squares to study covariation in shape. Syst. Biol. 49, 740–753.

Ross, C., Henneberg, M., 1995. Basicranial flexion, relative brain size and facial kyphosis in *Homo sapiens* and some fossil hominids. Am. J. Phys. Anthropol. 98, 575–593.

Ross, C., Ravosa, M., 1993. Basicranial flexion, relative brain size and facial kyphosis in nonhuman primates. Am. J. Phys. Anthropol. 91, 305–324.

Strait, D., 1999. The scaling of basicranial flexion and length. J. Hum. Evol. 37, 701–719.

Streissguth, A.P., Sampson, P., Barr, H., 1993. The Enduring Effects of Prenatal Alcohol Exposure on Child Development. University of Michigan Press, Michigan.

Szombathy, J., 1925. Die diluvialen Menschenreste aus der Fuerst-Johanns-Hoehle bei Lautsch in Maehren. Die Eiszeit 2, 1–34. pp. 73–95.

Udupa, J.K., 1999. 3DVIEWNIX 1.2. Department of Radiology, University of Pennsylvania Medical Center, Philadelphia, PA.

White, T.D., Folkens, P.A., 1991. Human Osteology. Academic Press, San Diego.

Woodward, A.S., 1921. A new cave man from Rhodesia, South Africa. Nature 108, 371–372.